

Finite Element Analysis of Single Sided Linear Induction Motor

Dr. Adil H. Ahmad* & Mehdi F. Bonneya*

Received on:22/6/2010

Accepted on:1/4/2010

Abstract

This paper presents analysis and operation of linear induction motor (LIM) using finite element method (FEM). The solution of magnetic field problem is performed for both two and three dimensional approaches. Magnetic vector potential, flux density, field intensity, induced rotor current, and propulsion force are computed for LIM model studied. The effect of velocity is taken into consideration. The primary winding self and mutual inductances are computed for three dimensional analysis.

Keywords- linear induction motor, finite element method, three-dimension analysis, ANSYS.

تحليلات العنصر المحدد لمحرك حثي خطي أحادي الجانب

الخلاصة

يتناول البحث تحليل وعمل محرك حثي خطي باستخدام طريقة العنصر المحدد. تم حل معادلات المجال المغناطيسي بكل من طريقة البعدين والثلاثة أبعاد. تم حساب متجه الجهد المغناطيسي , كثافة الفيض , شدة الفيض , تيار الحث للعضو المتحرك , وقوة الدفع للمحرك. تم اخذ تأثير السرعة بنظر الاعتبار في الحل, كما تم حساب المحاثة الذاتية والتبادلية لمفات العضو الابتدائي بواسطة التحليل الثلاثي البعد.

Introduction

Linear Induction Motor (LIM) is a non-conducting, high speed, linear motion operates on the same principles of rotary induction motors [1]. It can be obtained by an imaginary process of cutting a rotary motor along its radius from the center axis of the shaft to the external surface of the stator core and rolling it out flat. This special type of induction motor find wide applications in industrial such as transportation, conveyer systems, sliding door closer, actuators, material handling, pumping of liquid metal [2]. LIM consists of excitation element called the stator and induced current element called the rotor. The primary (stator) contains a three phase winding with uniform slots of the laminated iron core. These winding produce linearly traveling magnetic field.

The secondary (rotor) is either Ferro or nonferrous sheet metal, with and without solid or laminated back iron, used to complete the magnetic circuit. Due to the primary traveling field, a secondary current induced in the reaction plate. The

interaction between the induced current and the changing electromagnetic field will generate electromagnetic thrust on the plate where linear speed is produced [3]. Since there is no any physical coupling between the primary and the secondary, a silent operation is produced with reduced maintenance.

LIM can be classified depending on its constriction, as single sided linear induction motor in which only one primary one secondary are found, or, double sided linear induction motor, in which there are two primaries on the two sided of the secondary, is placed. Figure 1 shows the construction layout of single sided LIM. .

Several methods from both analytical and numerical techniques have been used to investigate, analyze, and optimize the operation of this type of induction motor. In this work finite element method is used for solution of magnetic field interior LIM domain using ANSYS software programming.

The mathematical model

The magnetic field equations can be solved by using two and three dimensional analysis. For two dimensional approach, the discontinuity of the motor in the direction of motion (x-axis) and the levitation direction (y-axis) is considered. The stator core extends into the x and y-direction, so that, the entry end effect and exit end effect of the motor are taken implicitly within the solution.

However the variation in the z-direction is not taken into account. The primary winding current is represented by actual slots representation.

For three-dimension analysis, the variation in physical quantities is taken into account in the solution, so that, most of the phenomena that exist in LIM are considered due to actual representation of the model that is considered in this type of analysis [4]. The effects of entry and exit end and the effects of width of both primary and secondary are shown also. However, this type of solution needs more time for solution.

The magnetic field in LIM is governed by Maxwell's equations in the general differential form where [5]:

$$\nabla \times \bar{H} = \bar{J} + \frac{\partial \bar{D}}{\partial t} \dots\dots\dots (1)$$

$$\nabla \cdot \bar{D} = r_c \dots\dots\dots (2)$$

$$\nabla \times \bar{E} = -\frac{\partial \bar{B}}{\partial t} \dots\dots\dots (3)$$

$$\nabla \cdot \bar{B} = 0 \dots\dots\dots(4)$$

Where $\bar{J}, \bar{H}, \bar{D}, \bar{B}, \bar{E}$, and r_c are current density, magnetic field intensity, electric flux density, magnetic flux density, electric field intensity, and volume charge density respectively.

In motor analysis, only quasi-static electromagnetic problems can be adopted. The time- derivative of current displacement can be neglected compared

to the current density, therefore, equation 1 is reduced to:

$$\nabla \times \bar{H} = \bar{J} \dots\dots\dots (5)$$

Applying that

$$\nabla \cdot \bar{J} = 0 \dots\dots\dots (6)$$

For an isotropic medium moving with velocity \bar{n} , the following equation holds:

$$\bar{J} = \bar{s}(\bar{E} + \bar{v} \times \bar{B}) \dots\dots\dots (7)$$

Introducing the magnetic vector potential \bar{A} , the following equations are added:

$$\bar{B} = \nabla \times \bar{A} \dots\dots\dots (8)$$

$$\bar{B} = \bar{m}\bar{H} \dots\dots\dots (9)$$

From equation 5 and 8 the following equations are obtained

$$\nabla \times \nabla \times \bar{A} = \bar{m}\bar{J}$$

$$\nabla(\nabla \cdot \bar{A}) - \nabla^2 \bar{A} = \bar{m}\bar{J}$$

$$\nabla \cdot \bar{A} = 0$$

$$\nabla^2 \bar{A} = -\bar{m}\bar{J} \dots\dots\dots (10)$$

$$\bar{E} = -\frac{\partial \bar{A}}{\partial t} \dots\dots\dots (11)$$

Substituting \bar{J} from equation 7 and using 11 gives [6]:

$$\nabla^2 \bar{A} = \bar{m}\bar{s}\left(\frac{\partial \bar{A}}{\partial t} - \bar{n} \times \nabla \times \bar{A}\right) \dots\dots(12)$$

This equation is the general field equation in terms of magnetic vector potential \bar{A} .

Taking into consideration these relations, then the LIM model can be divided into three main regions:

- The 1st region is the primary 3-ph winding where there is supply current density \bar{J} in this region, and then equation 10 is governing equation of this region.
- The 2nd region is rotor conducting plate where the velocity is taken into account, the governing equation is equation 12.

- The 3rd region is stator iron core, air gap and back iron region where there is no supply current density or eddy current induced, the governing equation is :

$$\frac{1}{m} \nabla^2 \bar{A} = 0 \dots\dots\dots (13)$$

The finite element matrix equation can be derived by using variational principles. These equations exist for linear and nonlinear material where magnetic vector potential formulation is applicable for both static and time varying magnetic field analysis with partial nonlinear permeability. The magnetic vector potential (called degree of freedom), element matrices, current densities can be put in matrices equation in the form of [7]:

$$[C]\{u\} + [K]\{u\} = \{J_i\} \dots\dots(14)$$

Where [C] and [K] are coefficient elements shape function matrices and equal to:

$$[C] = \begin{bmatrix} [C^{AA}] & [C^{AV}] \\ [C^{AV}]^T & [C^{VV}] \end{bmatrix} \dots\dots (14-a)$$

$$[K] = \begin{bmatrix} [K^{AA}] & [0] \\ [K^{AA}] & [0] \end{bmatrix} \dots\dots (14-b)$$

{u} is the unknown matrices for both A and time integral potential V given in the form of:

$$\{u\} = \begin{Bmatrix} \{A_e\} \\ \{V_e\} \end{Bmatrix} \dots\dots\dots (14-c)$$

{J_i} is current density in conducting element matrix and equal to:

$$\{J_i\} = \begin{Bmatrix} \{J^A\} \\ \{J^t\} \end{Bmatrix} \dots\dots\dots (14-d)$$

Where J^A source current density is vector and J^t is total current density vector

The element matrices and load vectors are presented for the most general cases of a vector potential analysis. For 2-D

analysis only one component of the magnetic vector potential A_x, A_y, and A_z are computed.

For 2-D time varying analysis, a current density load of either source {J_s} or total {J_t} current density is valid, where J_t represents the impressed current expressed in term of a uniformly applied current density .

For 3-D analysis, only source current density is allowed. After computing magnetic vector potential, then the evaluation is done for magnetic flux density B, which is defined as the curl of the magnetic vector potential:

$$\{B\} = \nabla \times [NA]^T \{A_e\} \dots\dots\dots (15)$$

Where:

{B} = Magnetic flux density

[NA] = Elements shape function

{A_e} = Nodal magnetic vector potential.

FEM forces computation

The magnetic forces in rotor plate are computed by elements using magnetic vector potential where three different techniques, are used to calculate magnetic forces at the element level.

The electromagnetic force is generally the superposition of the Laplace and the magnetic force [4]:

$$F = \int_v (J \times B) dvol - \int_v \left(\frac{1}{2} H^2 grad m \right) dvol \dots\dots(16)$$

The first term of the equation represents the electromagnetic force, which is the result of iteration between the electrical current density and the magnetic flux density. The second component is the magnetic force, which depends on the magnetization state of the body studied.

Magnetic forces in current carrying conductors can be computed by numerically integrating [7, 8]:

$$\{F\} = \int_{vol} \{N\}^T \{J\} \{B\} dvol \quad (17)$$

Where:

$\{N\}^T$ = Transport vector of shape functions.

Numerical analysis software

The software adopted in this work is ANSYS program to simulate LIM model using two and three dimensional analysis. The ANSYS program uses Maxwell's equations as the basis for magnetic field analysis. The primary unknown (degree of freedom) that the finite element solution calculates are magnetic vector potential A_x , A_y and A_z . Other magnetic field quantities are derived from these degrees of freedom which depend on element type, option and degree of freedom chosen.

ANSYS program has many finite element analysis capabilities starting simple, linear, nonlinear, and transient analysis. This software enables users to build computer models by using graphical user interface (GUI).

For two dimensional analysis, the variation is taken in both x and y axis while the variation in z axis is taken to be constant. The primary winding is simulated by massive conductor current. The rotor plate and back iron are created also by rectangular area, air gap and air enclosure the model is created. The rotor plate and back iron are build also by rectangular area, air gap and air enclosure the model are build in the same manner. The two dimensional model is shown in figure 2, the material properties of each part, defined by its relative permeability m_r , and electrical resistivity for nonferrous material both 3-phase primary winding and rotor plate. For permeability material region, define m_r for linear analysis, or specify $B-H$ curve reading from material library or by creating $B-H$ curve. Flux density B value

must be unique for each H value, and must monotonically increase with H . The $B-H$ curve should cover the complete operating range of the material. If a point beyond the end of the curve is required, the $B-H$ curve is extrapolated at constant slope.

The three dimensional analysis is performed using ANSYS workbench simulation program provides working environment for modeling and developing electromagnetic field analysis where typical tasks can be performed by creating models from a variety of computer-aided designs, conditioning models for design simulation and performing finite element analysis simulation. The workbench includes Design Modeler and Simulation of the analyzed LIM model.

Design modeling is used as a geometry editor of existing computer-aided design models. It is a parametric feature-based solid modeler designed so that the user can intuitively and quickly begin modeling three-dimensional engineering analysis preprocessing. All parts of the studied model are represented by its permeability and resistivity.

The winding bodies are special form of line bodies that are intended to model coils of wire. In fact, a normal line body can be converted to a winding body. The other way of winding bodies can be via winding tool. Winding bodies are created by the winding tool, cannot be converted to normal line bodies. Instead of having a standard cross section assigned to them, winding bodies currently only allow a rectangular cross section, and its values are determined by the winding table for winding bodies from the winding tool.

In order to apply the boundary conditions to field domain at the exterior faces, an enclosure for air will be created by using enclosure tool. The shapes of enclosure depends on the model shape

(box for LIM) and target all bodies, also, the depth of enclosure is defined. The enclosure feature supports symmetry models when the enclosure shape is a box or cylinder.

For electromagnetic analysis, the excitation is applied to the winding by defining the current magnitude and phase angles for phase A, B and C. The current applied to each phase remain constant during the solution (constant current source).

Magnetic flux boundary conditions impose constraints on the direction of the magnetic flux on the LIM boundary. This boundary condition may only apply to surfaces. By default, this feature restricts the flux to be normal to all exterior faces. A parallel flux is required to, at least, one surface of the simulation model. It is typically applied on the outer faces of the air body (enclosure) to contain the magnetic flux inside the simulation domain or symmetry plane surfaces where the flux is known to flow parallel to the surface of the analyzed model.

Results

The LIM model used for two and three dimensional analysis feed from constant current source for linear and nonlinear materials for computing all field quantities, forces, induced rotor currents, power losses, and other performances values.

In linear analysis, the Frontal Solution is used for model solution which is based on Gauss elimination. For two dimensional analysis, the applied magnetic model comprises 2362 elements and total number of nodes included in the model is 7111 using PLANE 53 for model simulation. For linear analysis, the permeability of Ferro materials is taken constant during the solution. The merit of this method of analysis is the effects of velocity, which can be introduced in the solution.

The primary result in this analysis is magnetic vector potential A_z for both real and imaginary computed values in the inter domain of the model using only nodal results. Magnetic field can be mapped by using vectors or contour distribution. The results of A_z simulation for model 1 are presented in figure 3 for zero velocity (m/sec) and 50 Hz frequency.

The effect of rotor velocity on the value and distribution of magnetic vector potential is shown in figure 4, where the distortions at both ends are clearly shown. The distribution of magnetic vector potential along the geometry dimension of the rotor can be plotted by select a defined path inside the middle of the rotor plate at certain nodes as shown in figure 5. Magnetic flux density value and its distribution inside this model is depicted in figure 6. The maximum value is shown in the stator teeth and gradually reduced in the pattern of poles flux lines.

Rotor induced current distribution inside the rotor plate element is shown in figure 7. These distributions indicate maximum positive direction and negative direction at the center of each pole.

The effect of rotor velocity is taken into consideration where the component of secondary current induced due to the rotor movement is shown in figure 8. This component value depends on rotor velocity.

Rotor propulsion force is computed in each element of the rotor in the direction of motion. The force distribution along the rotor length shows the maximum force values in rotor elements which are in front of poles center as shown in figure 9. This force is reduced at the half slot poles at the entry and exit end of the model. The propulsion force is in x-axis direction.

For three dimension solution, different types of rotor metal are considered where the flux density, intensity, winding self

and mutual inductances are computed. For aluminum plate, the flux density depicted in figure 10 at air gap 3.6 mm.

The flux density (x component) inside stator core is shown in figure 11.

The flux density (y component) inside stator core is shown in figure 12.

The field intensity distribution in rotor is depicted in figure 13 where the distribution depends on the pole position.

The self and mutual inductances of motor primary winding for aluminum rotor plate type shown in table 1 where the inductances values exhibited the difference between three phase winding inductance due to the end effects.

Another two types of rotor plate metal are studied, the first one is gray cast iron. For this type, the relative permeability is constant and equal to 1000, with electrical resistivity $9.6 \times 10^{-8} \Omega m$. The solution in this case is linear. The flux density is increased more than that for aluminum plate due to the high relative permeability of this type of metal. The self and mutual inductance for gray cast iron are shown in table 2 where its values exhibited higher values than that for aluminum plate type.

For silicon core iron rotor plate type where the relative permeability is depending on the B-H curve. The solution is nonlinear and the flux density is slightly more than that aluminum type.

The self and mutual inductance is slightly less than that for gray cast iron type as shown in table 3.

Conclusions

By making use of finite element analysis criteria, the field quantities are depicted inside any section of the model. For two dimensional analysis the magnetic vector potential A_z distribution at standstill and moving rotor are computed. The distribution of contour flux lines depends on the value of the magnetic vector potential at each

contour line. The highest value is near the center of the pole and the smaller contour value is in the outer direction of the pole center. Also, the sequence of pole polarity is positive and negative respectively. The value of A_z decrease with increasing rotor speed.

The magnetic flux density B distribution depends on the component and on real and imaginary parts of the defined component. The field intensity depends on the flux density value at the region that field intensity is computed and depends also on the type of material. For Ferro material (where the relative permeability is more than one). The value of field intensity is reduced in air gap and rotor plate. By using three dimensional solution, the above conclusion are confirmed where the field quantities distribution at every part of the model. The self and mutual inductances are computed where the effect of rotor metal has reasonable effects on both inductances and flux density inside model.

References

- [1]- D.Dolinar, G.Stumberger and B.Gracor "Calculation of the linear induction motor model parameters using finite elements" IEEE Transactions on magnetics, Vol. 34, No.5, September 1990.
- [2]- C. Huang and I. Chen, "Adaptive control approach for speed motion-sensorless of linear induction motor unknown resistance and payload" Proceeding of the 17th world congress, Korea, July 6-11, 2008.
- [3]- I. Boldea and S.A.Nasar "The induction machine Handbook" CRC press LLC 2002.
- [4]- A.H.Isfahani , B.M.Ebrahimi and H.Lesani " Design optimization of low-speed single-sided linear induction motor for improved efficiency and power factor " IEEE Transaction on magnetics ,Vol. 44, No.2 ,Feb. 2008.

[5]- Matthew N.O.Sadiku "elements of electromagnetics" published by Oxford University press, Inc. 2001.
 [6]- J.H.H.Alwash, J.A.H.Al-rekabi "Finite element analysis of linear induction machines" proc. IEE, vol. 126, No.7, July 1979.
 [7]- ANSYS "Element reference" Release 5.4, Swanson analysis, Inc. second edition.1997.
 [8]- F.T.Szabo, "Computing the force of linear machines using finite-element analysis ", Electrical machines parameters, 26 may, 2001.

Table (1) Motor winding inductances (aluminum rotor).

Coi l	A	B	C
A	5.587E-3	-1.38E-3	-2.25E-3
B	-1.38E-3	5.572E-3	-2.24E-3
C	-2.25E-3	-2.24E-3	5.55E-3

Table (2) Motor winding inductances (gray cast iron rotor).

Coil	A	B	C
A	7.197E-3	-1.84E-3	-3.10E-3
B	-1.84E-3	7.17E-3	-3.09E-3
C	-3.10E-3	-3.09E-3	7.16E-3

Table (3) Motor winding inductance (silicon core iron).

Coil	A	B	C
A	7.665E-3	-1.88E-3	-3.25E-3
B	-1.88E-3	7.653E-3	-3.24E-3
C	-3.25E-3	-3.24E-3	7.532E-3

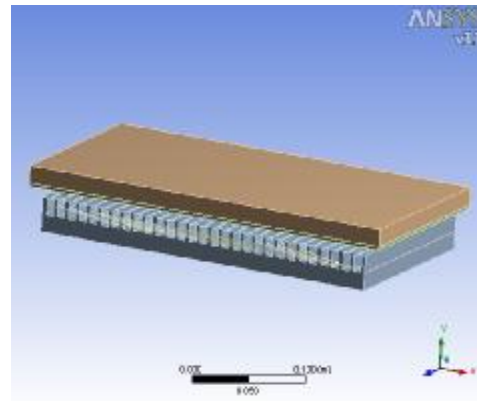


Figure (1) single sided LIM model under consideration.

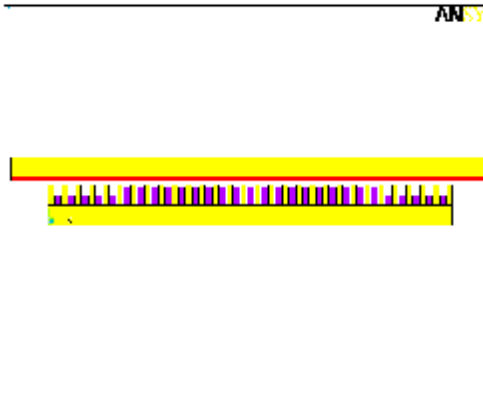
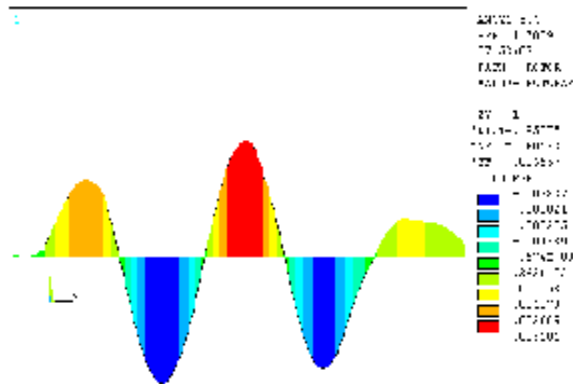


Figure (2) Two dimensional model.



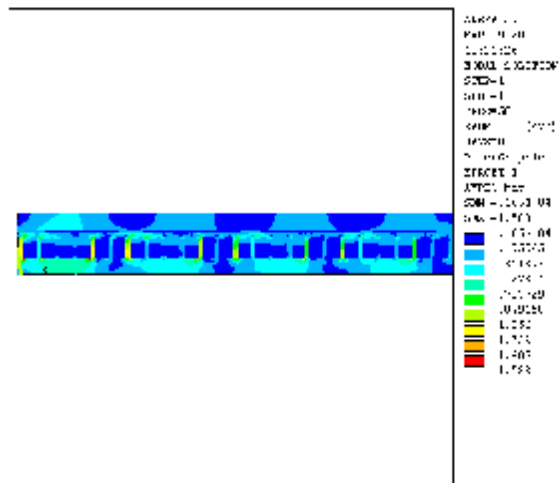
Figure(3) Magnetic vector potential at velocity=0, f=50 Hz.



Figure(5) Geometry plotting of magnetic vector potential at velocity=5, f=50 Hz.



Figure(4) Magnetic vector potential at velocity=5, f=50 Hz.



Figure(6) Contour plotting for flux density at velocity=5, f=50 Hz.

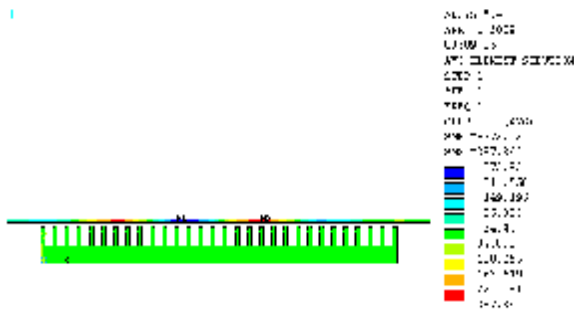


Figure (7) Rotor current distribution velocity=0, f=50 Hz.

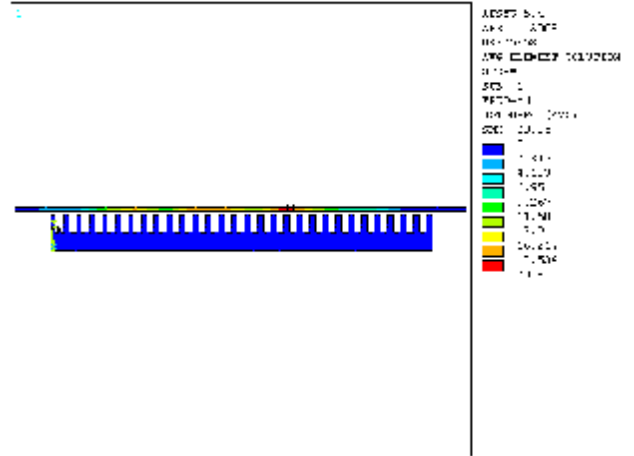


Figure (9) Rotor force velocity=5, f=50 Hz.

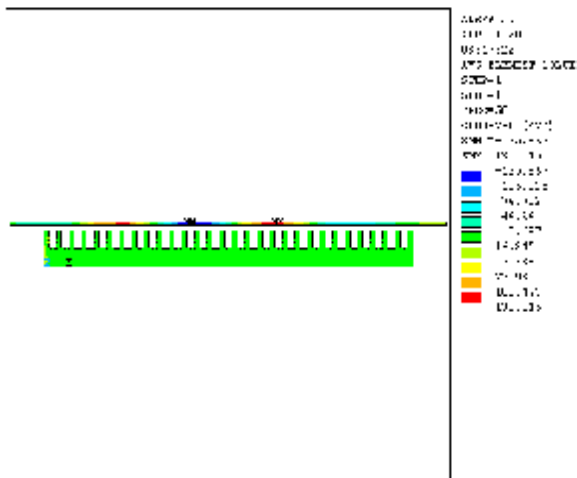
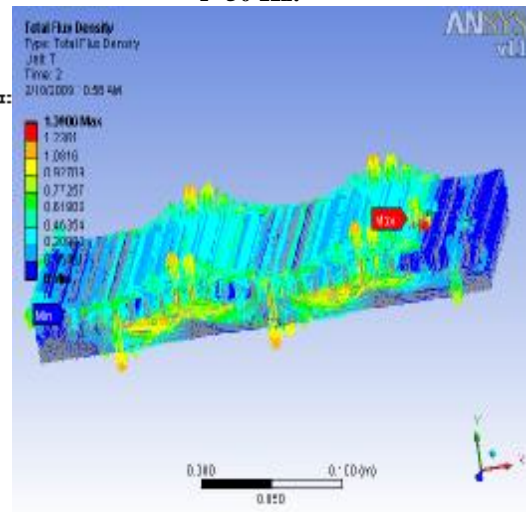


Figure (8) Velocity current component, velocity=5, f=50 Hz.



Figure(10) Flux density in stator using aluminum rotor.

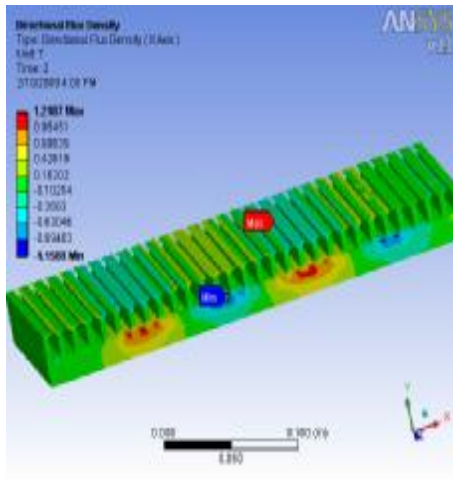


Figure (11) Flux density B-x in stator using contour plotting.

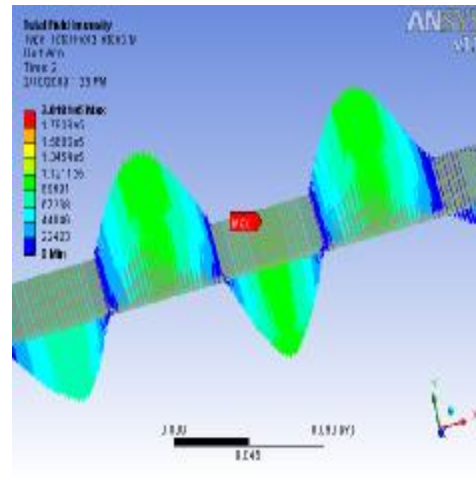


Figure (13) Field intensity in rotor

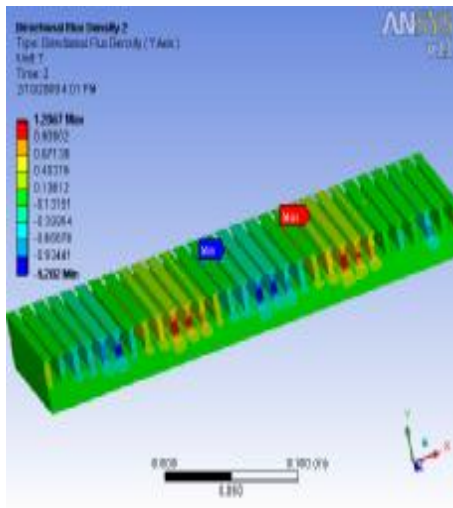


Figure (12) Flux density B-y in stator using contour plotting.